High signal contrast gating with biomodified Gd doped mesoporous nanoparticles†

Wen-Yen Huang, **Gemma-Louise Davies**, and **Jason J. Davis**[*]
Department of Chemistry, University of Oxford, South Parks Road, Oxford, OX1 3QZ, UK

Abstract

Internally Gd doped mesoporous nanoparticles have been prepared and exhibit unprecedented relaxivities that are retained on external biomodification. In tuning diffusive water access, image contrast can be reversibly switched in the presence of a specific protein target.

Among the spatially resolved clinical imaging modalities now available, magnetic resonance imaging (MRI) remains the most convenient and widely used of those which are non-invasive.[1] During the past decade a great deal of progress has been made in enhancing the natively low image contrast available within protic MRI relaxivity with molecular, biological or nanoparticle based formulations based on chelated gadolinium, through aggregation/rotation based changes or alterations in metal hydration number.[1,2] Such attempts include those which are biovectorable and thus capable of identifying and reporting on specific physiology and pathology.[3-11] A range of 1,4,7,10-tetraazacyclododecane-1,4,7,10-tetraacetic acid (DOTA) and diethylenetriaminepentaacetic acid (DTPA) derivatives have, for example, been bound to peptides, monoclonal antibodies or proteins capable of targeting specific cell receptors.[3,4,12]

Mesoporous silica nanoparticles (MSNs) offer much potential to both high contrast imaging and the delivery of therapeutics and can be chemically modified with relative ease.[13-17] Indeed, the chemical capping of MSNs has been investigated as a means of triggering drug delivery.[18] Particles <200 nm in size are generally believed to be able to avoid reticuloendothdlial system (RES),[19,20] an ability greatly aided through the use of masking hydrophilic coatings (*e.g.* polyethylene glycol; PEG).[21] To date, there exist several examples of doped MSNs capable of generating marked T_1 or T_2 contrast.[2,22] Notably, although central to any targetted imaging application, the effects of particle biomodification on this have not previously been considered. Since the diffusive access of water through particle nanopores to internalised magnetic elements is both theoretically expected[23,24] and experimentally[25,26] verified to underpin T_1 relaxivity (and thus image contrast), the initial motivation of this work was to generate <100 nm pegylated and biomodified nanoparticles with retained internal water access and high relaxivity. The ability of an external protein to

[*]jason.davis@chem.ox.ac.uk; Fax: +44 (0)1865 272 690; Tel: +44 (0)1865 275 914 .

selectively respond to specific partner proteins in solution was subsequently used to gate image contrast.

Silica nanoparticles are generally believed to be non-toxic *in vitro* and *in vivo*.[27] To avoid the known toxic risk associated with free Gd^{3+},[28] kinetically inert Gd–DOTA complexes were utilised herein.[29] We have previously demonstrated that the covalent tethering of these macrocycles to MSNs can be achieved with negligible Gd loss over a 4 week period[30] (also see below). The appendage of paramagnetic centres to MSNs instills not only advantages associated with increased rotational correlation time,[11] but also those engendered by the high surface area and water access features of a mesoporous scaffold,[23,25,26] yielding constructs with markedly high relaxivity.[24,25,30] In order to maximise the sensitivity of this to processes occurring on the outer surface of the particles we have biased the location of covalently bound Gd–DOTA internally (a space likely to be associated with restricted water mobility, increased diffusional (τ_D) and rotational (τ_R) correlation times and altered water proton residence lifetime (τ_m)[31-34]) through the use of a modified co-condensation procedure.[30,35] This methodology generates imaging agents with extraordinarily high relaxivities[30] (Fig. S1, ESI[†]).

Transmission Electron Microscope (TEM; Fig. 1 and Fig. S3, ESI[†]), dynamic light scattering (DLS; Fig. S2a, ESI[†]) and BET (Brunauer-Emmett-Teller; Fig. S2c, ESI[†]) surface area analysis data confirmed the native Gd doped MSNs (Gd–DOTA MSNs) to be well dispersed with a particle diameter of 75.9 ± 6.4 nm, hydrodynamic size of 138.7 nm (PDI: 0.09) and pore sizes of 3.2 ± 1.3 nm. Subsequent external surface modifications were conducted *via* the stepwise post-grafting of PEG layers (PEG5000 and PEG2000), a process monitored through associated changes in zeta potential (Fig. S2d, ESI[†]). The assessments confirmed these procedures to be highly reproducible and associated with negligible perturbation of particle stability/dispersion or size (Fig. S2a and S3, ESI[†]). Importantly, these surface modifications could also be achieved with negligible loss of MR relaxivity (Fig. S4a, ESI[†]), observations consistent with the high entropy, low packing density and water penetration characteristics of such layers. The effectiveness of subsequent protein modification in mediating clean particle vectoring to target proteins was analyzed in a microarray format on modified glass chips (Fig. S5, ESI[†]).

In seeking to analyse the effects of biomodification on particle MR contrast characteristics one may, in the first instance, consider the effects of the biomolecular layer on particle rotational correlation time τ_c (s) according to $\tau_c = (4\pi\eta r^3)/3kT$ where r is radius, η the solvent viscosity, (8.94×10^{-4} kg m^{-1} s^{-1} for H_2O at 298 K), and kT its usual meaning.[23] Herein, a ~6 nm biomolecular coat (BSA)[36] is expected to generate a negligible percentage change in τ_c (from ~3×10^4 ns to 9×10^4 ns).

Significantly, particle relaxivity can be tuned through the use of variable length spacer sitting between the natively hydroxylated surface and the anchored protein (Fig. 2). Specifically, the direct anchoring of BSA through a short linker (3-aminopropyl)-

triethoxysilane (APTES) leads to a $78.5 \pm 1.5\%$ drop in relaxivity, a reproducible observation we assign to the steric capping of particle pores and thus heavily restricted diffusional water access to internalised Gd centres. In inserting a PEG5000 spacer between the particle and protein, vectoring is enabled with retention of high relaxivity ($78.0 \pm 6.0\%$ of the non protein capped particle; Fig. 2).[37] Interestingly, the use of a shorter PEG2000 spacer leads to a reduced recovery of relaxivity (14.90 ± 0.56 mM^{-1} s^{-1}, $67.5 \pm 5.5\%$ of native value), an observation reflective of its inability to robustly keep the protein coat (tethered or otherwise) away from the particle pores (Fig. 2).

We have subsequently sought to use this steric gating in fabricating nanoparticles for which image contrast is reversibly switched by the presence or absence of a protein partner (Fig. 3). In establishing this proof of principal we have utilised the steric bulk of streptavidin (STV, 5 nm[38] > particle pore size, 3.2 ± 1.3 nm). In the first instance native Gd–DOTA doped MSNs were biotin modified with retention of facile water access (see detailed experimental procedures in ESI†). In the presence of low molar equivalents of streptavidin such particles could be robustly capped without aggregation or significant increase in resolved particle hydrodynamic radius[39-41] (see Fig. S1b, ESI†) but a dramatic (>60%) decrease in relaxivity (Fig. 3). The colloidal and relaxivity characteristics of these capped particles are unchanged through three months of storage in water (see Fig. S4c, ESI†), the latter observation, made after particle washing and centrifugation, being consistent with negligible leakage of Gd (the gating characteristics referred to below are also retained at 3 months).

In confirming the specificity of this image contrast capping, the relaxivity characteristics of biotinylated Gd-doped MSNs were unchanged in the presence of molecular biotin, biotin saturated STV or natively unmodified BSA (Fig. S4b, ESI†). Though the solution phase affinity of biotin for STV is very high,[38] a substantial size dependent decrease in this at nanoparticle surfaces has been previously noted as has the competitive displacement of STV by solution phase biotin.[38,41,42] In the presence of 1000 fold excess (7 μM) of biotinylated BSA, the gating STV is displaced and particle relaxivity recovers to $84.5 \pm 8.5\%$ of its original value) (Fig. 3). [Note that, because of the very low biotin coverages (<1 biotin unit per 1000 nm^2 of particle surface) employed in this work, we do not expect potentially displacement hindering multivalent/local concentration effects.][42-44]

In conclusion, the synthesis of colloidally stable, protein capped and vectoring Gd doped MSNs is reported herein. Through appropriate surface chemistry, these can be externally modified without detrimental loss of very high relaxivity (39.26 ± 1.29 mM^{-1} s^{-1} at 3 T, unprecedented for nanoparticles based on a silica scaffold).[30,45] Significantly, the Gd loading can be internally biased at the point of synthesis such that diffusive water access, and hence MR contrast, can be sterically gated at the particle periphery. While the integration of suitably long PEG spacers enables protein conjugation to be achieved with retention of an "open gate", conjugation with short spacers dramatically reduces relaxivity. In the presence of solution phase protein partners these sterically bulky protein gates are competed off and high image contrast returns. Though there exist examples of paramagnetic contrast agents for which contrast has been ionically or biologically tuned through a change in hydration number or rotational correlation time (see Table S1, ESI†), the work herein not

only identifies and utilises the importance of water access, but also constitutes the first example of reversible T_1 contrast gating exploiting protein recognition. This proof of principal, and an array of potential derivatives, is of significant potential value in furthering the application of nanoparticle chemistry to functional MR imaging.

Supplementary Material

Refer to Web version on PubMed Central for supplementary material.

Acknowledgments

Notes and references

1. Huang WY, Davis JJ. Dalton Trans. 2011; 40:6087–6103. [PubMed: 21409202]

2. Kim J, Piao Y, Hyeon T. Chem. Soc. Rev. 2009; 38:372–390. [PubMed: 19169455]

3. De Leon-Rodriguez LM, Ortiz A, Weiner AL, Zhang SR, Kovacs Z, Kodadek T, Sherry AD. J. Am. Chem. Soc. 2002; 124:3514–3515. [PubMed: 11929234]

4. Lauffer RB, Brady TJ. Magn. Reson. Imaging. 1985; 3:11–16. [PubMed: 3923289]

5. Moats RA, Fraser SE, Meade TJ. Angew. Chem., Int. Ed., Engl. 1997; 36:726–728.

6. Li WH, Fraser SE, Meade TJ. J. Am. Chem. Soc. 1999; 121:1413–1414.

7. Lowe MP, Parker D, Reany O, Aime S, Botta M, Castellano G, Gianolio E, Pagliarin R. J. Am. Chem. Soc. 2001; 123:7601–7609. [PubMed: 11480981]

8. Nivorozhkin AL, Kolodziej AF, Caravan P, Greenfield MT, Lauffer RB, McMurry TJ. Angew. Chem., Int. Ed. 2001; 40:2903–2906.

9. Caravan P, Cloutier NJ, Greenfield MT, McDermid SA, Dunham SU, Bulte JWM, Amedio JC, Looby RJ, Supkowski RM, Horrocks WD, McMurry TJ, Lauffer RB. J. Am. Chem. Soc. 2002; 124:3152–3162. [PubMed: 11902904]

10. Breckwoldt MO, Chen JW, Stangenberg L, Aikawa E, Rodriguez E, Qiu SM, Moskowitz MA, Weissleder R. Proc. Natl. Acad. Sci. U. S. A. 2008; 105:18584–18589. [PubMed: 19011099]

11. Major JL, Boiteau RM, Meade TJ. Inorg. Chem. 2008; 47:10788–10795. [PubMed: 18928280]

12. Guo HX, Yang HQ, Gallazzi F, Prossnitz ER, Sklar LA, Miao YB. Bioconjugate Chem. 2009; 20:2162–2168.

13. Luo Z, Cai KY, Hu Y, Zhao L, Liu P, Duan L, Yang WH. Angew. Chem., Int. Ed. 2011; 50:640–643.

14. Climent E, Bernardos A, Martinez-Manez R, Maquieira A, Marcos MD, Pastor-Navarro N, Puchades R, Sancenon F, Soto J, Amoros P. J. Am. Chem. Soc. 2009; 131:14075–14080. [PubMed: 19739626]

15. Schlossbauer A, Kecht J, Bein T. Angew. Chem., Int. Ed. 2009; 48:3092–3095.

16. Zhu CL, Lu CH, Song XY, Yang HH, Wang XR. J. Am. Chem. Soc. 2011; 133:1278–1281. [PubMed: 21214180]

17. Zhu CL, Song XY, Zhou WH, Yang HH, Wen YH, Wang XR. J. Mater. Chem. 2009; 19:7765–7770.

18. Saha S, Leung KCF, Nguyen TD, Stoddart JF, Zink JI. Adv. Funct. Mater. 2007; 17:685–693.

19. Lin YS, Abadeer N, Haynes CL. Chem. Commun. 2011; 47:532–534.

20. Fan J, Fang G, Zeng F, Wang X, Wu S. Small. 2012 DOI: 10.1002/smll.201201456.

21. Rio-Echevarria IM, Selvestrel F, Segat D, Guarino G, Tavano R, Causin V, Reddi E, Papini E, Mancin F. J. Mater. Chem. 2010; 20:2780–2787.

22. Tong S, Hou SJ, Zheng ZL, Zhou J, Bao G. Nano Lett. 2010; 10:4607–4613. [PubMed: 20939602]

23. Caravan P, Ellison JJ, McMurry TJ, Lauffer RB. Chem. Rev. 1999; 99:2293–2352. [PubMed: 11749483]

24. Takahara S, Sumiyama N, Kittaka S, Yamaguchi T, Bellissent-Funel MC. J. Phys. Chem. B. 2005; 109:11231–11239. [PubMed: 16852371]

25. Carniato F, Tei L, Dastru W, Marchese L, Botta M. Chem. Commun. 2009:1246–1248.

26. Taylor KML, Kim JS, Rieter WJ, An H, Lin WL, Lin WB. J. Am. Chem. Soc. 2008; 130:2154–2155. [PubMed: 18217764]

27. Barnes CA, Elsaesser A, Arkusz J, Smok A, Palus J, Lesniak A, Salvati A, Hanrahan JP, de Jong WH, Dziubaltowska E, Stepnik M, Rydzynski K, McKerr G, Lynch I, Dawson KA, Howard CV. Nano Lett. 2008; 8:3069–3074. [PubMed: 18698730]

28. Oksendal AN, Hals PA. J. Mag. Res. Imag. 1993; 3:157–165.

29. Wang XY, Jin TZ, Comblin V, Lopezmut A, Merciny E, Desreux JF. Inorg. Chem. 1992; 31:1095–1099.

30. Davis JJ, Huang W-Y, Davies G-L. J. Mater. Chem. 2012; 22:22848–22850.

31. Ananta JS, Godin B, Sethi R, Moriggi L, Liu X, Serda RE, Krishnamurthy R, Muthupillai R, Bolskar RD, Helm L, Ferrari M, Wilson LJ, Decuzzi P. Nat. Nanotechnol. 2010; 5:815–821. [PubMed: 20972435]

32. Fries PH, Belorizky E. J. Chem. Phys. 2010; 133:024504. [PubMed: 20632760]

33. Aime S, Frullano L, Crich SG. Angew. Chem., Int. Ed. 2002; 41:1017–1019.

34. Sethi R, Ananta JS, Karmonik C, Zhong M, Fung SH, Liu X, Li K, Ferrari M, Wilson LJ, Decuzzi P. Contrast Media Mol. Imaging. 2012; 7:501–508. [PubMed: 22991316]

35. Cauda V, Schlossbauer A, Kecht J, Zurner A, Bein T. J. Am. Chem. Soc. 2009; 131:11361–11370. [PubMed: 19722649]

36. Anderegg JW, Beeman WW, Shulman S, Kaesberg P. J. Am. Chem. Soc. 1955; 77:2927–2937.

37. The ~20% relaxivity decrease is assigned to the physisorption of non covalently coupled BSA to non sterically protected areas of the particle surface during the biomodification steps.

38. Piletska EV, Piletsky SA. Langmuir. 2010; 26:3783–3785. [PubMed: 20151674]

39. Muller W, Ringsdorf H, Rump E, Zhang X, Angermaier L, Knoll W, Spinke J. J. Biomater. Sci., Polym. Ed. 1994; 6:481–495. [PubMed: 7841153]

40. Li M, Wong KKW, Mann S. Chem. Mater. 1999; 11:23–26.

41. Aslan K, Luhrs CC, Perez-Luna VH. J. Phys. Chem. B. 2004; 108:15631–15639.

42. Duan XX, Li Y, Rajan NK, Routenberg DA, Modis Y, Reed MA. Nat. Nanotechnol. 2012; 7:401–407. [PubMed: 22635097]

43. Myung JH, Gajjar KA, Saric J, Eddington DT, Hong S. Angew. Chem., Int. Ed. 2011; 50:11769–11772.

44. Hong S, Leroueil PR, Majoros IJ, Orr BG, Baker JR, Holl MMB. Chem. Biol. 2007; 14:107–115. [PubMed: 17254956]

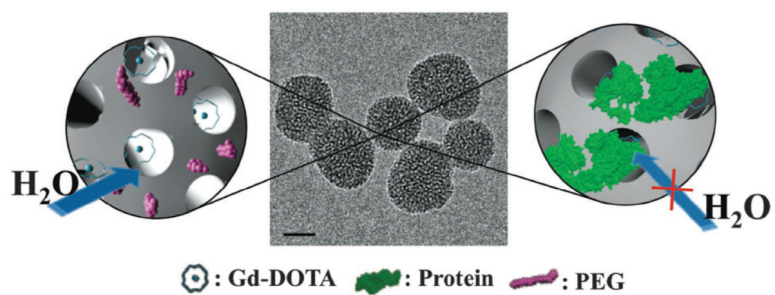45. Taylor-Pashow KML, Rocca JD, Lin W. Nanomaterials. 2011; 2:1–14. [PubMed: 24527205]

Fig. 1.
TEM image of representative protein capped Gd–DOTA MSNs (75.9 ± 6.4 nm in diameter; scale bar 50 nm). The schematics depict the native pegylated (left) and sterically capped (right) water access to internalised Gd–DOTA units.
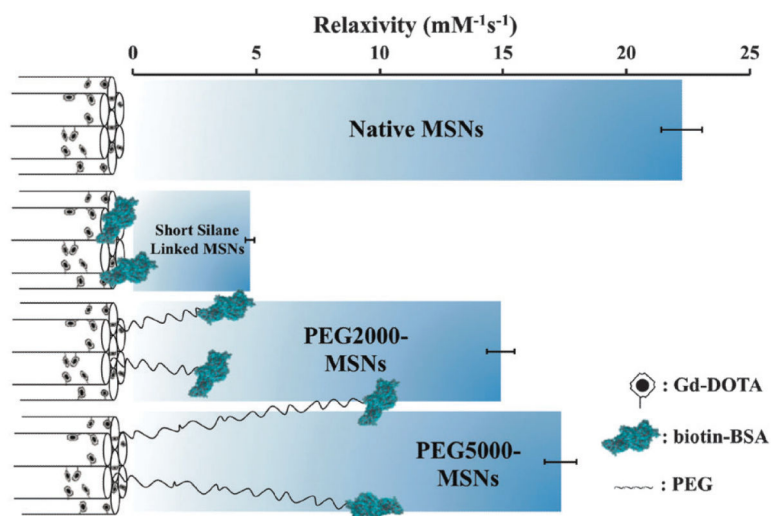
Fig. 2.
Schematic summary of particle relaxivity tuning through surface chemistry. Non protein capped Gd–DOTA MSNs have open pores, good water accessibility and relaxivities of 22.25 ± 0.83 mM^{-1} s^{-1} in water; the direct anchoring of BSA *via* a short silane linker leads to a dramatic reduction in relaxivity (4.74 ± 0.18 mM^{-1} s^{-1}); in buffering this biomodification away from the surface with a linker, high relaxivity is recovered (14.90 ± 0.56 mM^{-1} s^{-1} for PEG2000, 17.34 ± 0.65 mM^{-1} s^{-1} for PEG5000). Error bars here represent cumulative errors arising from triple repeats of relaxivity assessment (across at least three different sample concentrations at 7 T and 20 °C) and ICP quantification.
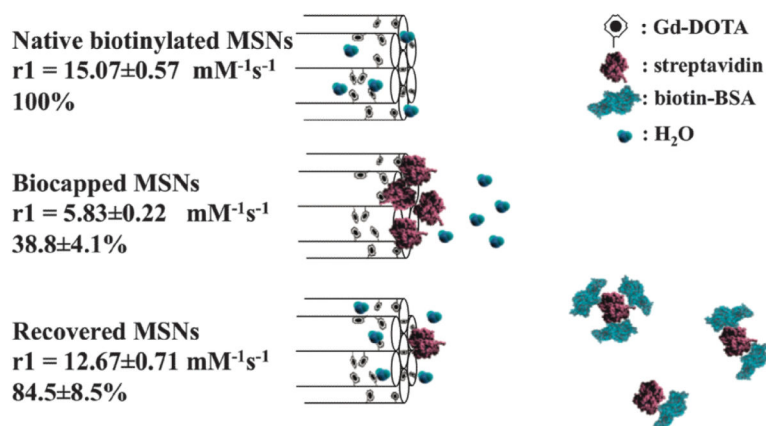
Native biotinylated MSNs
r1 = 15.07±0.57 mM^{-1}s^{-1}
100%

Biocapped MSNs
r1 = 5.83±0.22 mM^{-1}s^{-1}
38.8±4.1%

Recovered MSNs
r1 = 12.67±0.71 mM^{-1}s^{-1}
84.5±8.5%

⬢ : Gd-DOTA
: streptavidin
: biotin-BSA
● : H$_2$O

Fig. 3.
Schematic summary of MSN relaxivity gating. Externally biotinylated Gd-doped MSNs enjoy good water accessibility and a high relaxivity (15.07 ± 0.57 mM^{-1} s^{-1}) that can be reversibly capped by the steric bulk of a bound STV (5.83 ± 0.22 mM^{-1} s^{-1}; <40% of the original value). In the presence of low µM biotinylated BSA, the gating protein is competed off the particle surface and relaxivity recovers to 12.67 ± 0.71 mM^{-1} s^{-1} ($84.5 \pm 8.5\%$ of original value). Error here represents cumulative error arising from triple repeats of relaxivity assessment (across at least three different sample concentrations at 7 T and 20 °C) and ICP quantification.